JSS Focus Issue on Advanced Interconnects: Materials, Processing, and Reliability

Modification of Ultra Low-k Dielectric Films by O_2 and CO_2 Plasmas

Teju Tunde Olawumi,[a,b] Elisabeth Levrau,[a,c] Mikhail Krishtab,[a] Christophe Detavernier,[a,c] Johann W. Bartha,[a,b,*] Kaidong Xu,[a] Frederic Lazzarino,[a,z] and Mikhail R. Baklanov[a]

[a]*IMEC, Kapeldreef 75, B-3001 Leuven, Belgium*
[b]*Institute of Semiconductors and Microsystems (IHM), TU Dresden, Germany*
[c]*Department of Solid State Sciences, COCOON, Ghent University, Ghent, Belgium*

Low-k materials developed for ULSI interconnects should have sufficient resistance to processing plasma. CO_2 plasma is being considered as a promising candidate for low damage photoresist ash and as a surface activation chemistry for self-assembled monolayers and atomic layer deposition on low-k materials. This article explores the interaction of two organosilicate (OSG) based low-k materials with different k-values (OSG2.4 and OSG2.2) with CO_2 plasma in both CCP and ICP-remote plasma chambers. Time dependent exposure of the materials to CO_2 plasma revealed quick and effective sealing of OSG2.4 surface whereas it takes longer time for OSG2.2. The sealing reduces further plasma damage and leads to accumulation of CO_2 in the pores of both materials. The same behavior occurs in ICP–remote plasma but without a complete sealing of the surface. This suggests the important role of ion bombardment. Damage to low-k by conventional O_2 plasma was studied alongside and it was found that for $t < 60$ s, O_2 plasma exerts more damage on OSG2.2 than CO_2. This trend is reversed at $t > 60$ s. Furthermore, lesser time exposure to CO_2 plasma was investigated with respect to source power at constant pressure and it was discovered that damage although small, increases with varying source power.

Manuscript submitted July 31, 2014; revised manuscript received October 10, 2014. Published October 18, 2014. *This paper is part of the JSS Focus Issue on Advanced Interconnects: Materials, Processing, and Reliability.*

The performance enhancement of electronic circuits was majorly centered on reducing the transistor sizes, increasing transistor speed and density. However, in advanced technology nodes the performance of the resulting integrated circuits (IC) is greatly hindered by the resistance – capacitance (RC) delay experienced during the signal propagation within the interconnects.[1] In order to solve this problem, the traditional Al was replaced by Cu, which has lower resistivity and SiO_2 with $k = 4.0$ was replaced by low dielectric constants (low-k) materials. Organosilicate glasses (OSG) deposited by Plasma Enhanced Chemical Vapor Deposition (PECVD) and/or by Spin-on Glass technology (SOG) are presently the most popular low-k materials.

Photoresist strip using O_2 based plasma is a conventionally used processing technique but this has been found to be severely damaging to porous low-k materials. The modifications to the porous low-k materials lead to increased k-values from densification and hydrophilization.[2–5] The CO_2-based plasma has been reported to be less damaging with respect to the O_2 counterpart. Fuller et al. proposed the use of CO_2 based RIE plasma for photoresist stripping.[6] Ming-Shu Kuo et al. and Hualiang Shi extensively studied the surface modification of ultralow-k materials by CO_2 plasma and the results are published in their PhD dissertations[7,8] and in several papers.[9–13] They reported that i) CO_2 and O_2 plasma damage to ultralow-k films are comparable ii) there is lower atomic oxygen density in CO_2 discharge than O_2 discharge because of higher activation energy (11.5 eV) required to liberate atomic oxygen from CO_2 than from O_2 molecules (6 eV) – this is why there is supposedly a reduction in damage by CO_2 discharge with respect to O_2 for same operating conditions iii) the ashing rate of CO_2 increases with the addition of Ar at higher pressure (about 100 mTorr) than at lower pressure hence the addition of Ar is beneficial and dependent on pressure. Adding Ar brings about the dilution of the concentration of O_2 atoms that are liberated from CO_2 hence a lower damage to low-k. In this article, we study the underlying mechanism behind the reduction in plasma damage by CO_2 plasma in comparison to O_2 plasma based on the phenomena of surface sealing and never-before reported trapping of CO_2 gas within the pores of ultralow-k films and in addition recommend an optimized CO_2 plasma recipe for low-k surface activation for the growth of self-assembled monolayers (SAMs).

For this study, two low-k films, OSG 2.4 and OSG 2.2 deposited by different methods, and with different k-values and porosities have been evaluated to understand the effects of CO_2 based plasma chemistry on these films. For comparison to existing plasma treatments, O_2 plasma experiments were also carried out. The experiments were carried out in an industrial dual frequency Capacitively-Coupled Reactive Ion Etching (CCP-RIE) chamber and in a home built Inductively-Coupled remote plasma (ICP-remote) chamber with varying times of plasma exposure or varying plasma power.

Experimental

The OSG materials with different porosities and k-values were deposited on 300 mm Si wafers using PECVD technology with broadband UV-assisted thermal curing (OSG 2.4)[14] and Spin-on technology (OSG 2.2). The SOG films were periodic mesoporous organosilicates (PMO), which are considered as possible candidates for future technology nodes because the application of self-assembly approaches and chemistries allows the control of properties and characteristics to a certain extent.[15–17] Their properties, evaluated by using different techniques are presented in Table I.

Plasma treatment was done in a CCP-RIE chamber of the TEL Tactras (from Tokyo Electron Limited) with a dual frequency source (40 MHz and 13.56 MHz) coupled to the bottom electrode. The top electrode instead of being RF biased, consists of a DC bias and a matching circuit which provides a superposition of the RF source and the DC source producing a negative DC voltage which is applied to the top electrode thus generating high energy ballistic electrons accelerated toward the opposite bottom electrode which is RF powered. CO_2 or O_2 gases were allowed into the chamber at 1200 SCCM, with 500W HF power and no substrate bias. The chamber pressure was 55 mT and the wafers were maintained at room temperature approximately 22°C. The damage by CO_2 and O_2 plasma on the low-k films was also studied in a ICP-remote plasma chamber equipped with an in situ transmission mid-IR spectrometer.[18] The inner chamber configurations of the CCP-RIE and ICP- remote plasma chambers used are as shown in

*Electrochemical Society Active Member.
[z]E-mail: Frederic.Lazzarino@imec.be

Table I. Overview of the properties of the used low-k films.

Low-k films	Deposition method	Thickness (nm)	RI @633 (nm)	k-value	Young's modulus (GPa)	Porosity (%)	Pore radius (nm)
OSG 2.4	PECVD	300	1.35	2.45	8.4	22	0.8
OSG 2.2	SOG	200	1.28	2.28	5.7	32	1.4

Figure 1. Spectroscopic Ellipsometry was done using F5_SCD (KLA Tencor) or a Wollam M-2000U to obtain the pre-treatment and post-treatment thickness and refractive indexes. Ex-situ transmission FTIR spectra were obtained using Nicolet 6700 spectrometer equipped with a closed compartment constantly purged with nitrogen flow to eliminate traces of atmospheric moisture and CO_2. A prototype design ellipsometer, EP 10 was used to carry out ellipsometric porosimetry (EP) measurements.[19] EP measurements were carried out using toluene as adsorbate. With increasing pressure, toluene vapor condenses in the open pores and the condensate amount is calculated from the change in refractive index by using the Lorentz-Lorentz equation.[19,20] Further characterization was done using a dual beam configured TOF-SIMS IV tool from ION-TOF GmbH and negative TOFSIMS depth profiles were recorded on a series of samples in order to get information about the depth of damage caused by a particular plasma treatment. The hydrophilic properties of the films after plasma treatment were also evaluated by water contact angle measurement. The 2 μm × 2 μm surface morphology images were recorded by the Agilent 5100 AFM/SPM microscope in tapping mode and then used for calculation of the root mean squared roughness (RMS).

Results and Discussion

Exposure in CCP-RIE plasma chamber.— The low-k films deposited on Si were cleaved into 35 mm × 35 mm sized coupons and glued with a thin layer of thermal joint paste (Wakefield 120) on to TiN wafers which served as both carrier and to observe the effects of the plasma conditions. The selection of TiN layers was argued by the fact that TiN layers are used as hard mask during the patterning and therefore, they mimic the real patterning condition. Right after the plasma exposure the samples were detached from the carrier wafer and the sample back-side was cleaned from the thermal joint residues with isopropanol before further characterization.

Low-k modification: FTIR data.—Several samples of the two low-k films have been exposed to different plasma exposure times from 2 s up to 150 s of CO_2 plasma in a CCP-RIE chamber on the TEL Tactras. Figure 2 shows the results of the ex-situ FTIR measurements of OSG 2.4 and OSG 2.2. The spectra of the two films are quite similar indicating similar compositions of the films. The vibrating band 950 – 1250 cm^{-1} can be attributed to the Si-O bonds which constitute the skeleton of the ultra-porous films.[21] The small changes of the left shoulder of this Si-O band suggest the formation of a SiO_2-like material from the Si-O network due to the plasma exposures.[22] The peak at 1275 cm^{-1} representing the hydrophobic $SiCH_3$ terminal groups in the films is decreasing with increasing plasma exposure time. Plasma treatments actually remove the hydrophobic $SiCH_3$ surface groups and replace them with hydrophilic Si-OH surface groups. The vibration band around 3700 cm^{-1} is attributed to these Si-OH surface groups that absorb moisture generated during the reaction or from the atmosphere after the experiment. The more $SiCH_3$ groups are converted to Si-OH groups, the more moisture can be absorbed in the film and hence the moisture content increases with increasing plasma exposure. This increase is more pronounced in OSG 2.2 than OSG 2.4 confirming our earlier assertion of higher porosity and larger pore size in OSG 2.2. Interestingly, a sharp peak around 2341 cm^{-1} attributed to CO_2 gas can be observed for both films suggesting the trapping of CO_2 molecules within the pores of the films as a result of the plasma treatment. While a steady and continuous increase in intensity of trapped CO_2 molecules is observed in OSG 2.4 (Figure 2c), it was observed that the CO_2 molecules trapped in the OSG 2.2 attain saturation point after 105 s exposure and then a drop in intensity of trapped gas is seen. It is not immediately understood why this phenomenal difference in the two materials occurs but it is assumed to be a result of stress relaxation in the densified top layer which leads to appearance of small cracks breaking the surface sealing and releasing the trapped CO_2 molecules. The mechanism was suggested by F. Bailly et al. to describe surface roughening of OSG films subjected to fluorocarbon plasmas.[23] However unlike the case of fluorocarbon plasmas the formed cracks may not result in surface roughening but in creation of extra paths for penetration of radicals damaging the bulk of seemingly sealed porous film.

To underscore our research study in understanding CO_2 as a lesser damaging gas for stripping, the low-k films have been exposed to O_2 plasma. Figure 3 shows the ex-situ transmission FTIR spectra of OSG 2.4 and OSG 2.2 before and after O_2 plasma exposures. The vibration absorption peak assigned to $SiCH_3$ (1275 cm^{-1}) shows a substantial intensity decrease with increasing plasma exposure indicating appreciable damage to the low-k film by the O_2 plasma treatment. At the same time moisture uptake increases showing again that the $SiCH_3$ surface groups are exchanged by Si-OH surface groups. Similar to the CO_2 plasma experiments, at 2341 cm^{-1}, a sharp peak attributed to CO_2 gas is surprisingly observed from the spectra indicating the

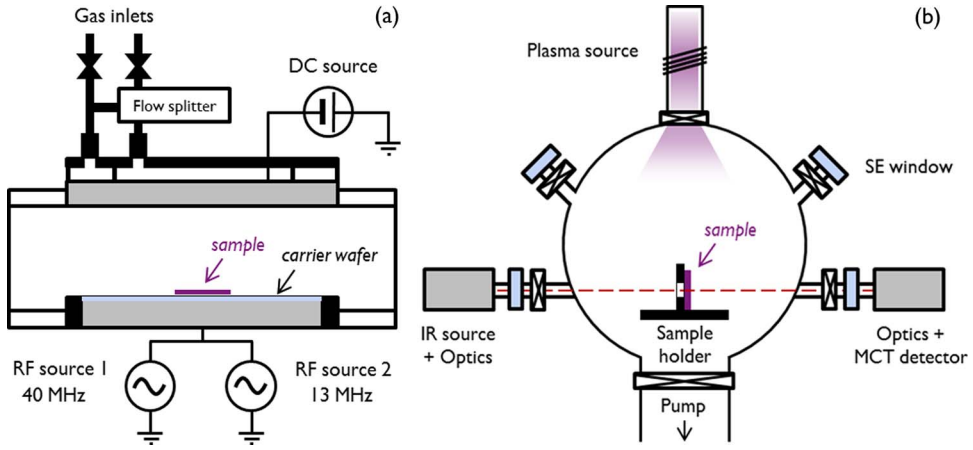

Figure 1. Schematic representation of the (a) dual-frequency CCP-RIE chamber and sample placement during the experiment and b) ICP-remote plasma setup equipped with in-situ transmission FTIR module.

trapping of CO_2 molecules within the pores of the low-k film following O_2 plasma treatment. Figure 3 also shows the comparison of the loss of $SiCH_3$ surface groups and CO_2 trapped in the pores of OSG 2.4 and OSG 2.2 in O_2 plasma. In O_2 plasma contrary to observations in CO_2 plasma, a difference in the behavior of the two films with respect to CO_2 trapping is observed. The plasma exposure results in a saturation and subsequent reduction in amount of CO_2 molecules trapped within the two films with the highest accumulation occurring for both films at 105 s.

To quantify the content of methyl groups in the material and their loss as a measure of plasma damage we used Si-CH_3 peak area divided by the area of Si-O peak and relative change of this ratio with respect to the value calculated for pristine material, respectively. Multiplied by the film thickness, the latter provides an estimate of plasma damage which can be regarded as effective thickness of damaged layer (EDL), i.e. a layer free of Si-CH_3 groups. By definition, it takes the thickness of the OSG layer into account and can be used to compare damage in OSG-2.2 and OSG-2.4 of different thickness. As shown in Figure 4a, the initial 2 s plasma pulse removes $SiCH_3$ surface groups very intensively but after that the additional decrease measured slows down for both low-k films. It is worth noticing that the level of damage in OSG-2.2 and OSG-2.4 materials differs only at the initial stage while at longer treatment times in CO_2-plasma the extent of damage and rate of its propagation is nearly the same or even slightly higher for the less porous OSG-2.4. Lower values of EDL in case of OSG-2.4 during the first 30–60 s can be related to its smaller pore size limiting the radical diffusion[2] and accelerating sealing of top surface as will be further discussed, while higher damage at longer exposure time can be explained by formation of shallow cracks in the stressed top layer of the film which allow penetration of damaging plasma species inside the pores. Nonetheless lower pore connectivity within the densified surface layer of OSG-2.4 makes it possible to retain most of the CO_2 gas trapped at the initial stages of exposure to CO_2-plasma. Similar trend of increasing damage with exposure

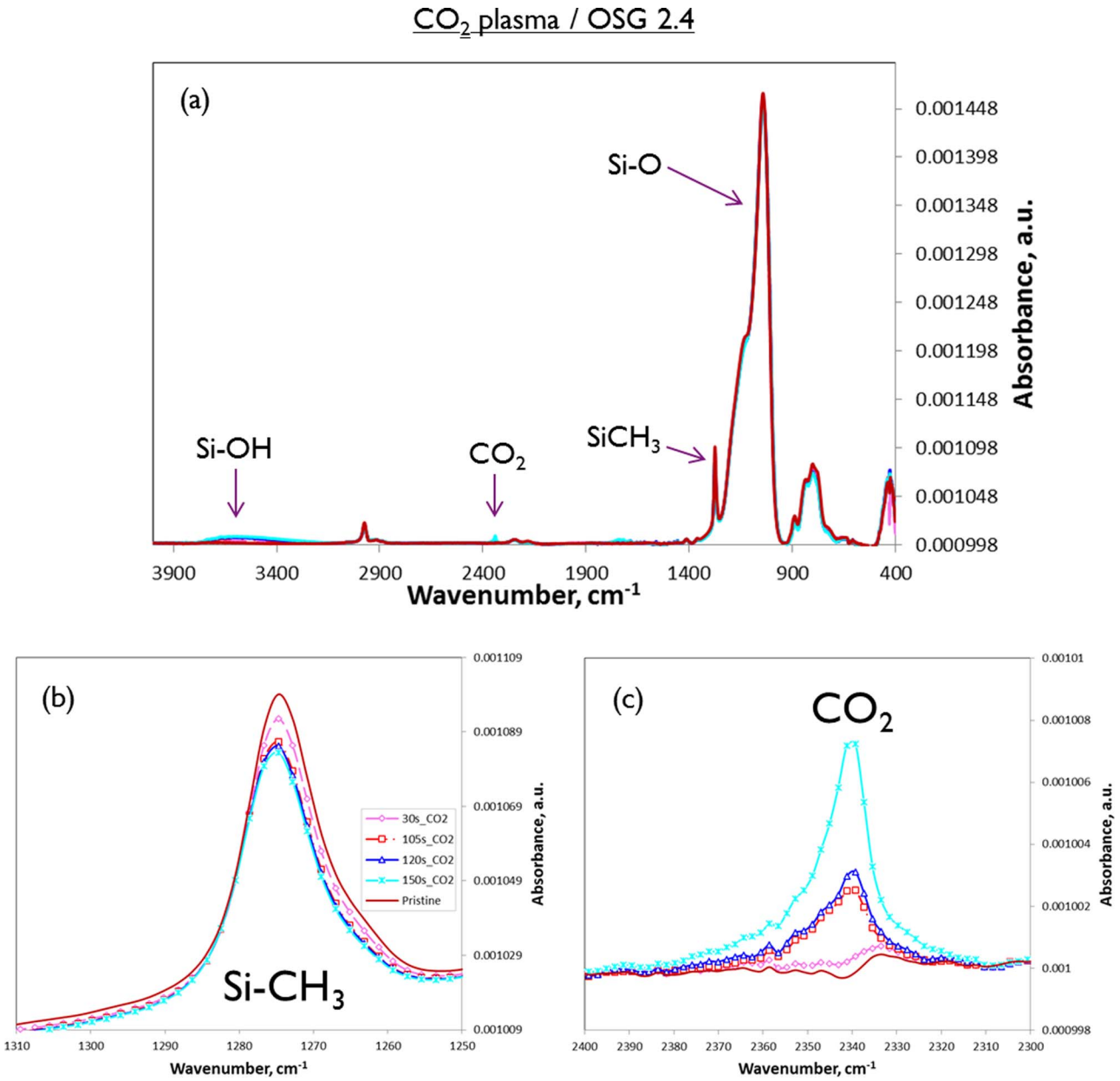

Figure 2. (Color Online) Ex-situ transmission FTIR spectra of OSG 2.4 showing a) full spectra, b) $SiCH_3$ surface groups, c) CO_2 trapped within the pores and OSG 2.2 showing d) full spectra, e) $SiCH_3$ surface groups, f) CO_2 trapped within the pores after exposures to CO_2 plasma in a CCP-RIE plasma chamber. The spectra were normalized to Si-O-Si peak located at ≈1063 cm^{-1}.

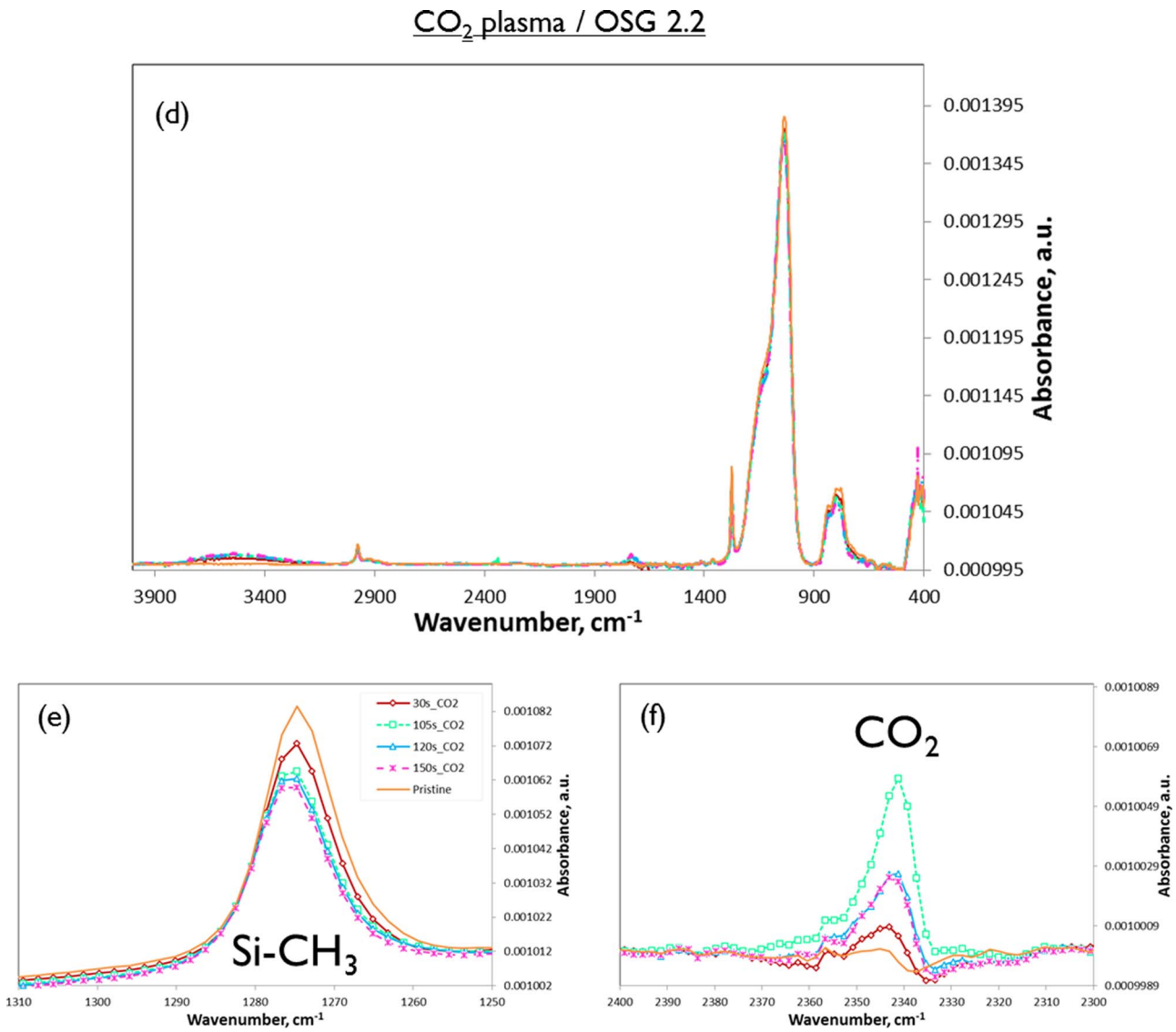

Figure 2. (*Continued.*)

time is observed for O_2 plasma, as shown in Figure 4b, although the damage induced by O_2 plasma is higher than damage induced by CO_2 plasma at short exposure times, which is again related to the rate of surface densification in the tested plasmas. Another interesting phenomena to be mentioned is that, for exposure times, $t < 60$ s, the $SiCH_3$ depletion in O_2 plasma is greater than CO_2 plasma but at $t > 60$ s, there is a flip in damage recorded as the low-k film experience more damage by CO_2 than by O_2 plasma. As discussed above, it can be attributed to the cracking of stressed top surface of OSG-2.2 under more prominent ion bombardment present in the case CO_2 discharge.

These experiments show that CO_2 and O_2 RIE plasmas modify both OSG 2.4 and OSG 2.2, breaking $SiCH_3$ bonds and converting them to Si-OH bonds. The degree of conversion increases with increasing time of exposure and OSG 2.2 has higher susceptibility to $SiCH_3$ bond breaking particularly during the first minute of exposure to the plasma due to its larger pore size and higher porosity. O_2 plasma induces more damage at lower pulse times whereas CO_2 damages more at higher pulse times. Moisture is absorbed and CO_2 gas is trapped within the pores of both films with both plasma treatments and a higher number of molecules were present in the OSG 2.2 film as compared to the OSG 2.4 film.

Change of porosity.—The low-k films were characterized with EP before and after both plasma treatments in the CCP-RIE plasma chamber. Figure 5 shows the EP data for OSG 2.4 and OSG 2.2 after both CO_2 and O_2 CCP plasma treatments. One can see that pristine OSG 2.4 had an open pore volume of about 22%, while pristine OSG 2.2 has open pore volume of 32% (Table I). OSG 2.4 was completely sealed after 5 s exposure to CO_2 plasma. Some delay in the adsorption and desorption curves is already observed after 2 s suggesting formation of a densified top layer and toluene penetration through this layer is diffusion limited (partial sealing) (Figure 5a). For OSG 2.2, 60 s CO_2 plasma exposure was necessary to partially seal the pores and 90 s for complete sealing (Figure 5b).

For the oxygen plasma treated samples (Figures 5c and 5d), partial and full sealing occurs for OSG 2.4 after 5 s and 10 s O_2 plasma, respectively. On the other hand, for OSG 2.2, partial and full sealing occurs at 90 s and ~120 s respectively. Evidently, it is due to the smaller pore size and higher density, that sealing occurs quite early for OSG 2.4 but the larger pore sized and highly porous OSG 2.2 experiences late sealing. Kunnen et al. have already reported low-k sealing by oxygen plasma in CCP plasma chamber.[24] Here, we compared our results of O_2 plasma with CO_2 plasma and it is observed that CO_2 plasma is more efficient for pore sealing in CCP chamber.

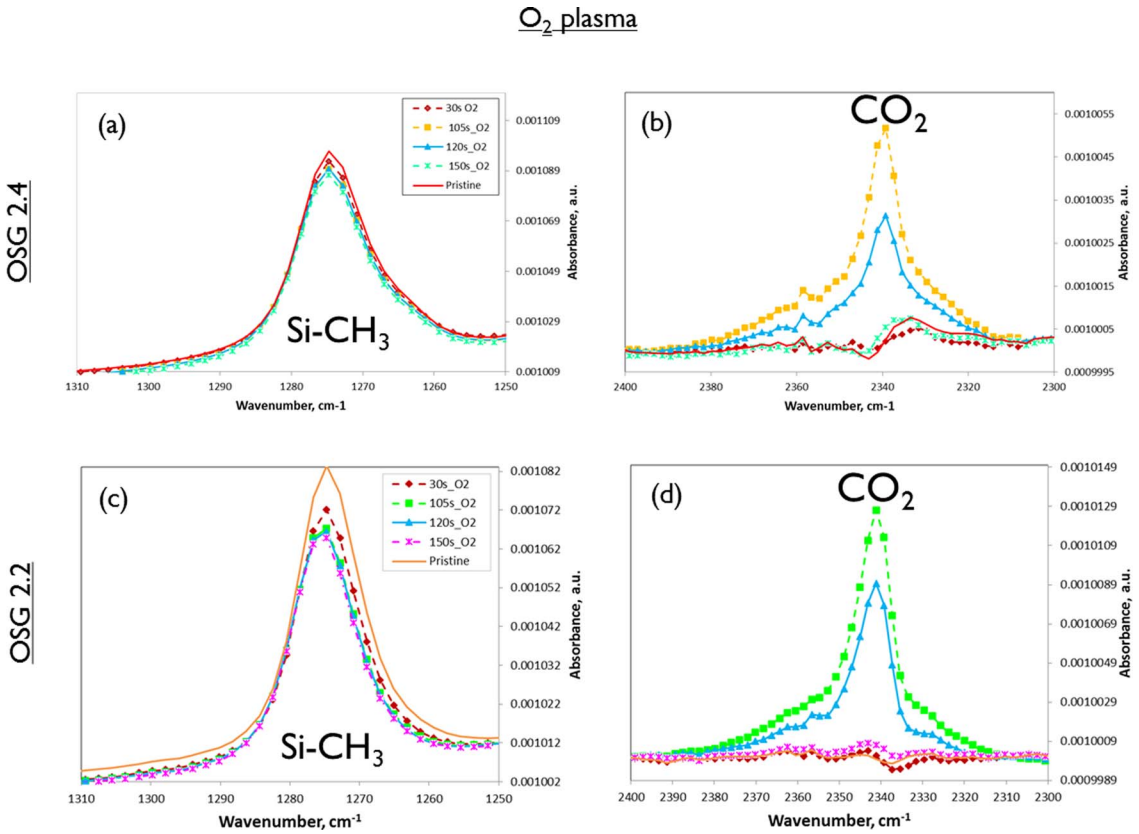

Figure 3. (Color Online) Ex-situ transmission FTIR spectra of OSG 2.4 showing a) $SiCH_3$ surface groups, b) CO_2 trapped within the pores and OSG 2.2 showing c) $SiCH_3$ surface groups, d) CO_2 trapped within the pores after exposures to O_2 plasma in a CCP-RIE plasma chamber. The spectra were normalized to Si-O-Si peak located at ≈1063 cm^{-1}.

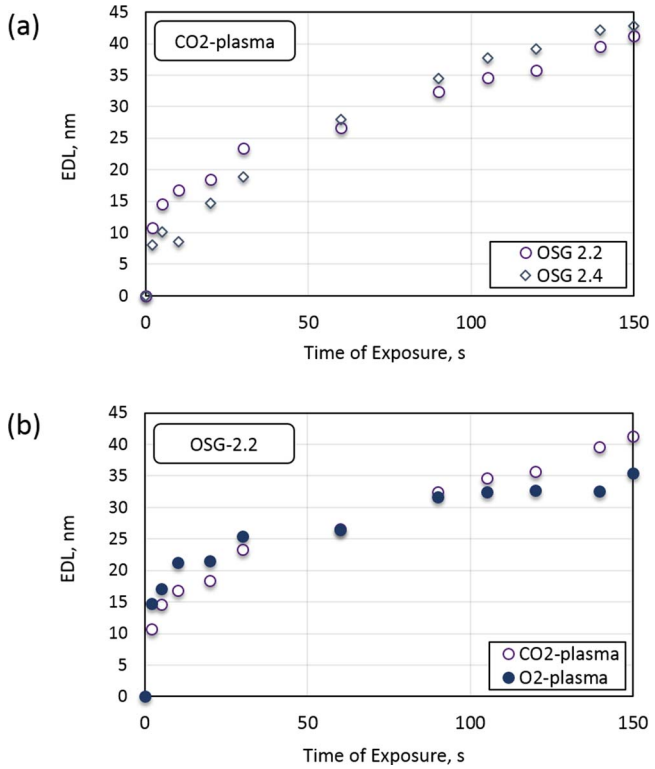

Figure 4. (Color online) Effective thickness of damaged layer (EDL) for a) OSG 2.4 and OSG 2.2 after CO_2 plasma and b) OSG 2.2 after O_2 and CO_2 plasma treatment.

Surface morphology.—The surface roughness of pristine low-k films and those exposed to CO_2 and O_2 plasmas is shown in Figure 6. One can notice that the dynamic of RMS changes agrees well with the FTIR and EP data. Similarly to discussion in the FTIR section, two stages of roughness evolution in case of OSG-2.2 during plasma treatment can be distinguished. At first roughness of the layer increases due to collapse of pores at the surface. Then the film gets smoother demonstrating RMS values lower than that of pristine film due to material densification driven by both cross-linking of newly formed silanols and momentum transferred by ions impinging the surface. Apparently duration of the first stage depends on the average pore size which is almost twice as large in the case of OSG-2.2. This could explain why the first "roughening" step is not seen in the Figure 6 for the less porous OSG-2.4. One can assume that it occurs at shorter treatment times (<30 s) not evaluated in this work. Generally lower values of RMS measured on the samples exposed to CO_2-plasma confirm important role of ion bombardment in faster sealing of porous surface of OSG-2.2 and OSG-2.4.

Depth profile of carbon concentration.—In order to visualize the depth of damage within the films, time of flight secondary ion mass spectroscopy (TOF-SIMS) measurements were carried out on the CO_2 and O_2 treated samples of the OSG 2.4 film. In Figure 7, TOF-SIMS intensities of carbon and SiO_2 clusters are plotted as a function of thickness for OSG 2.4. The thickness scale was obtained based on peak in Si-profile corresponding to silicon substrate and thickness of the OSG film pre-measured by ellipsometry thus assuming uniform sputtering rate of the low-k dielectric layer.

The results show that pristine low-k film had a small carbon depleted area near the top surface but the bulk carbon concentration is uniform. Both CO_2 and O_2 plasmas deplete carbon. The most intensive carbon depletion in near surface area happens during the first

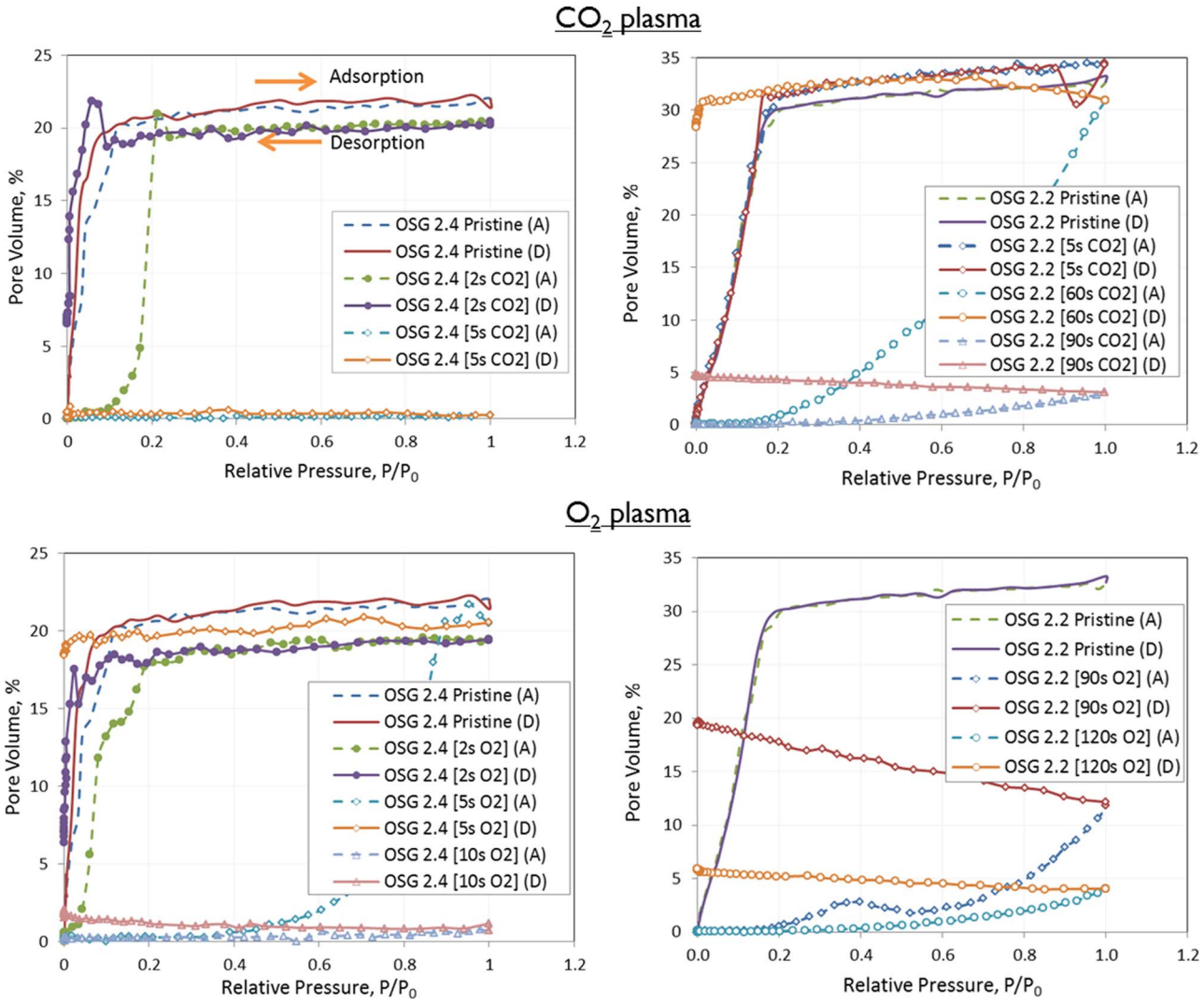

Figure 5. (Color online) Ellipsometric Porosimetry for OSG 2.4 after (a) CO_2, (c) O_2 and OSG 2.2 after (b) CO_2, (d) O_2 CCP-RIE plasma treatments.

5 s. Both CO_2 and O_2 plasmas reduce carbon concentration by two orders of magnitude. The depth of damage is about 15–20 nm in both cases.

The longer exposure demonstrates principal difference between these two plasmas. In the case of CO_2 plasma further reduction of carbon concentration near the top surface is observed while the depth of damage remains unchanged. In the case of O_2 plasma, in addition to reduction of surface carbon concentration, significant damage propagation into the film is observed. After 60 s exposure, the depth of damage was about 75 nm.

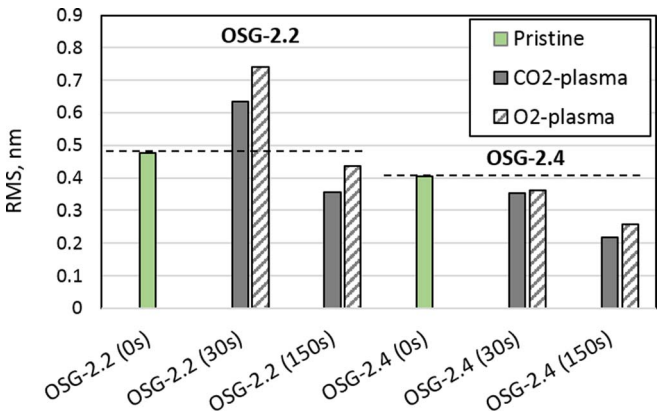

Figure 6. (Color online) Surface roughness (RMS) measured by AFM on OSG-2.2 and OSG-2.4 samples exposed to CO_2 and O_2 plasmas.

It is interesting that FTIR analysis shows almost same total carbon depletion in CO_2 and O_2 plasmas (Figure 4). Therefore, the conclusions based on characterization of total carbon depletion sometimes can be not sufficient for complete understanding of modification mechanisms.

Effect of plasma power on OSG 2.2.—The low power CO_2 plasma is considered as a promising method for selective surface modification for SAMs deposition on low-k films.[25] Normally a short time exposure in low power CO_2 plasma is used for this purpose and this is the reason why the effect of the plasma power on the damage induced on OSG 2.2 was investigated for 2 s exposure to plasma. Stability and reproducibility of the discharge was checked by monitoring of OES spectra. The lowest tested level of RF power (50 W) resulted in steady optical emission spectra after about 1.5 s. Shorter plasma stabilization delays are expected for the conditions with higher RF power applied. From ex-situ FTIR measurements, the normalized $SiCH_3$ removal as a function of plasma power was derived. The result is plotted in Figure 8. First, there is a high amount of $SiCH_3$ groups removed from the surface at a plasma power of 50 W. Between 50 W and 200 W, the amount of $SiCH_3$ groups removed stays constant. After 200 W, there is again a strong removal followed by saturation at 400 W – 500 W.

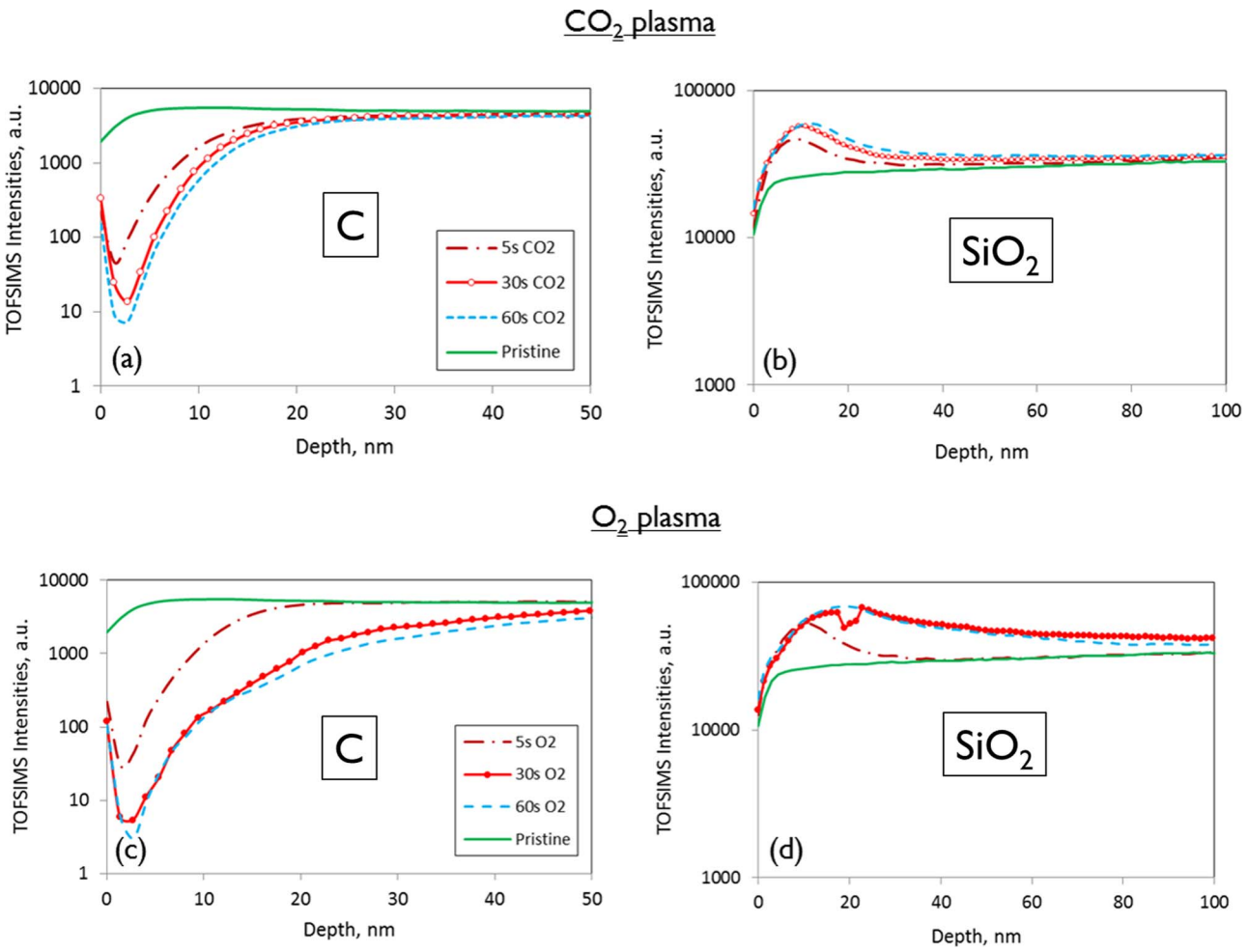

Figure 7. (Color online) OSG 2.4 TOF-SIMS measurements obtained for carbon [a, c] and SiO_2 [b, d] after CO_2 plasma [a, b] and O_2 plasma [c, d] treatments.

Ex-situ mid-IR was used to examine the moisture uptake as a result of CO_2 plasma exposures at different plasma power and compared to O_2 plasma. The results are presented in Figure 9. The moisture uptake increases with increasing plasma power and it is always higher in the wafers exposed to O_2 plasma in comparison with CO_2 plasma confirming our earlier results of the higher damaging effect of O_2 plasma.

The dependence of integral plasma damage on power is obvious. The degree of damage is very small at 50 W power that is normally used for surface treatment before SAMs deposition. However, if this damage were uniformly distributed in low-k film, the surface hydrophilization might be not sufficient. To shed more light on this question, the water contact angle (WCA) measurements on the film before and after CO_2 plasma treatments are shown in Figure 10. With the exposure to plasma, the WCA decreases from 99° to about 21° for 50 W plasma power and about 3° for subsequent increase in plasma power. The low-k surface is converted from hydrophobic to hydrophilic even at very low power (50 W). Therefore, even at very low total damage, the top surface has already been transformed into hydrophilic state. This is a requirement for the selective growth of SAMs on surface of

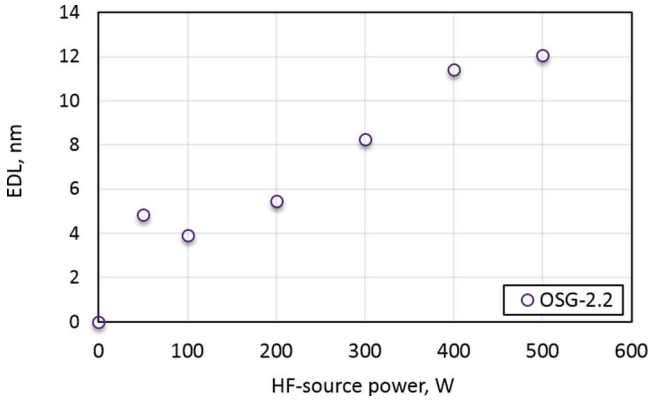

Figure 8. FTIR data: Effective thickness of damaged layer (EDL) for OSG 2.2 after exposure to varying CO_2 plasma powers.

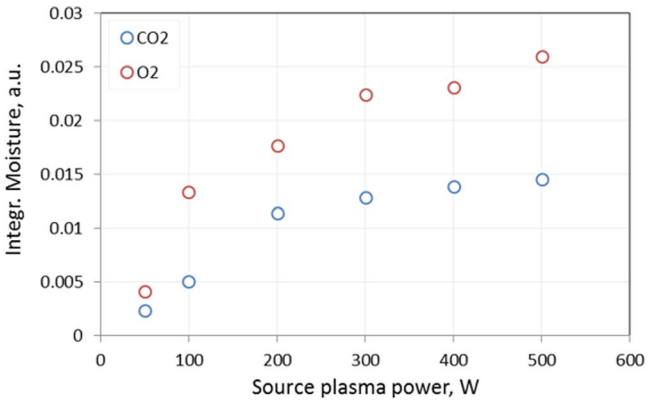

Figure 9. (Color online) FTIR data: integrated moisture uptake by OSG 2.2 after CO_2 plasma treatment at varying plasma powers.

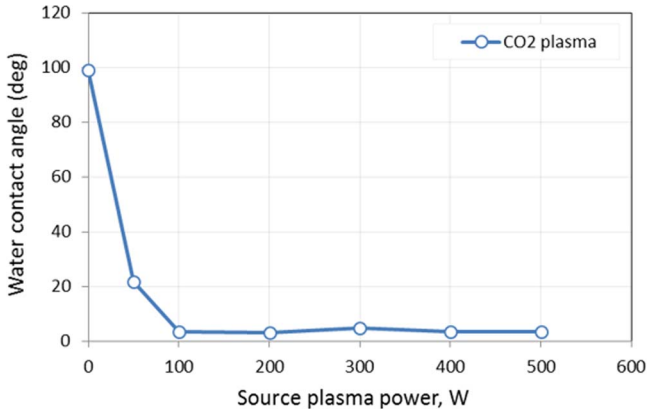

Figure 10. Water contact angle of OSG 2.2 film after CO_2 plasma exposure.

OSG-based low-k films and for appropriate wetting of pore stuffing material in post porosity plasma protection approach.[26]

Based on the provided results, it is proposed that a 2 s, 55mT, 50/100 W CO_2 plasma is sufficient to make the surface of ultralow-k films hydrophilic as these conditions provide the least damage to the material i.e. the least C depletion.

Exposure in ICP-remote plasma chamber.— The reactor configuration setup at CoCooN (Ghent University) is shown in Figure 1b. The OSG 2.4 and OSG 2.2 films were exposed to 2, 5, 20 and 30 s of CO_2 and O_2 plasma at room temperature under the following conditions: 5 mTorr pressure, 126 SCCM gas flow rate and a 200 W LF (13.56 MHz) remote plasma source. Samples represented by pieces of silicon substrate with a layer of low-k material were mounted vertically in the chamber using a 5 cm × 4 cm rectangular sample holder to allow in situ transmission mid-IR measurements. In this configuration, the samples are exposed to radicals and VUV photons only but suffer no ion bombardment in contrast to the CCP-RIE chamber where the sample surface is exposed to all three species. This setup and plasma condition makes the experiments performed in the ICP-remote plasma chamber somewhat milder than in the CCP-RIE chamber.

All spectra for both plasma treatments on the films showed similar peak changes but the spectra of OSG 2.4 after up to 30 s CO_2 is shown in Figure 11. The $SiCH_3$ peak is decreasing with increasing plasma exposure and the material becomes more SiO_2-like. No moisture adsorption or CO_2 trapping is observed in this configuration. Since these experiments were done under softer plasma conditions and the measurements were performed in situ, the little moisture or CO_2 that is formed can be pumped away immediately. Plotting the EDL as a function of plasma exposure time (Figure 12) shows again that OSG 2.2 is more susceptible to CO_2 damage than OSG 2.4 because of porous structure differences. The $SiCH_3$ depletion in OSG 2.4 is already saturated after 5 s, while 30 s is not even sufficient to saturate OSG 2.2. The difference between the CO_2 and the O_2 plasma damage is less pronounced than in the CCP-RIE plasma chamber.

EP measurements of these samples show significant reduction in porosity of the low-k films after plasma exposure as shown in Figure 13. For the treatment of the two OSG films in both CO_2 and O_2

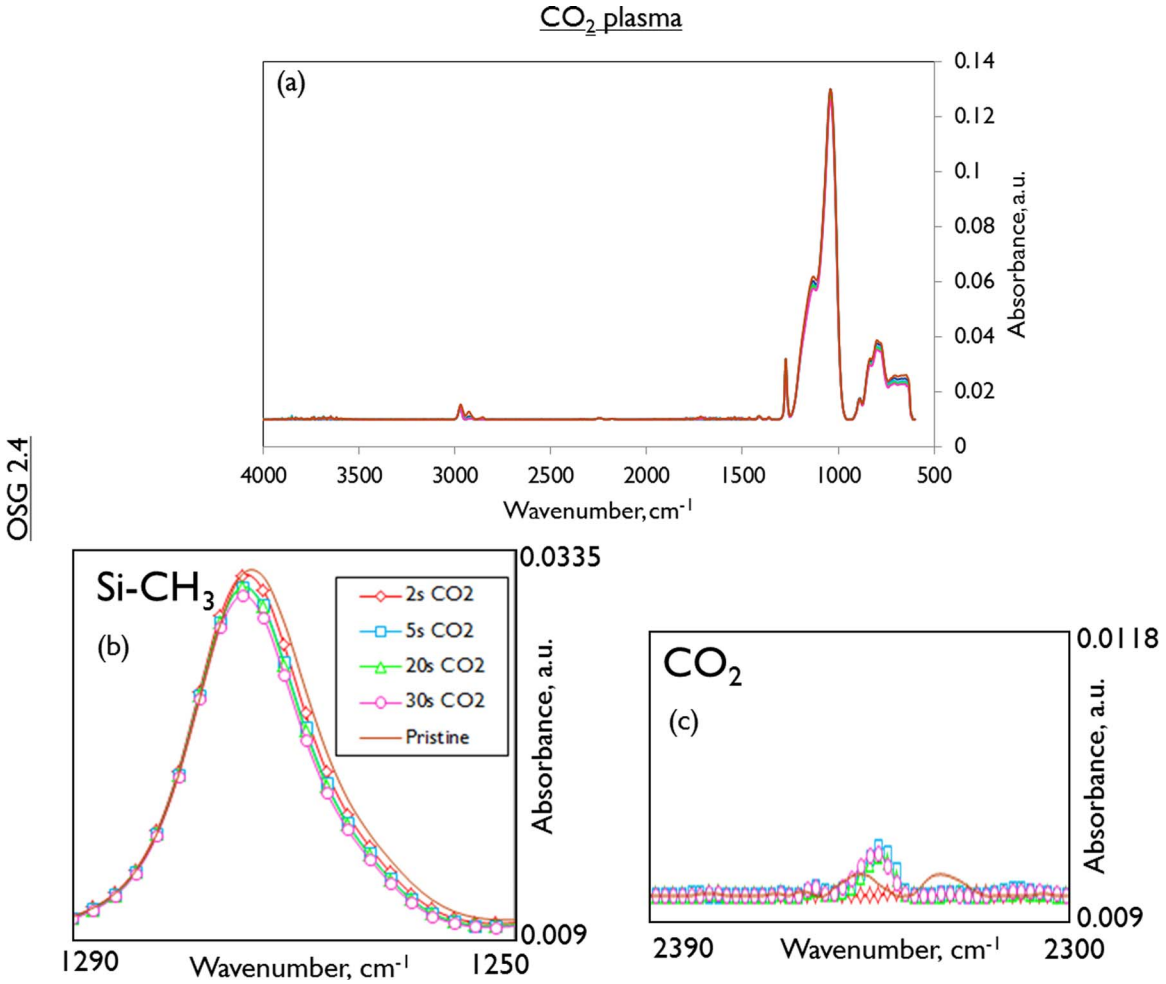

Figure 11. (Color online) FTIR Spectra of OSG 2.4 (a) Full spectra, (b) $SiCH_3$ peaks and (c) CO_2 peaks after ICP-remote CO_2 exposure.

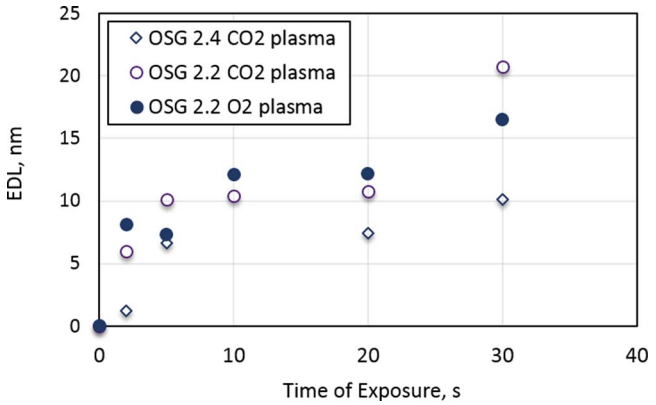

Figure 12. Effective thickness of damaged layer (EDL) for OSG 2.4 after CO_2 plasma and OSG 2.2 after CO_2 plasma and O_2 plasma.

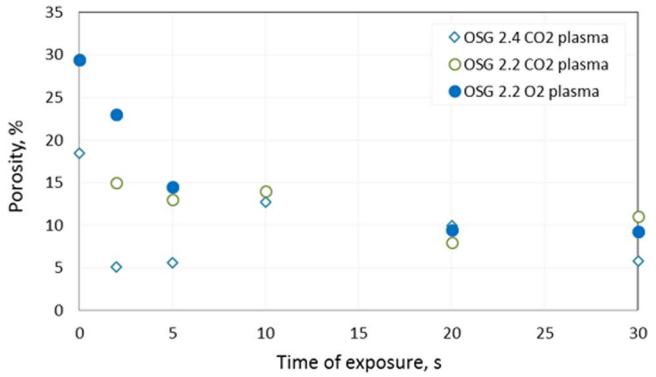

Figure 13. (Color Online) EP data for OSG 2.4, OSG 2.2 after CO_2 plasma and OSG 2.2 after O_2 plasma treatments in ICP-remote plasma chamber.

plasma, open porosities of the materials reduced with increased time of plasma exposure achieving only partial sealing during up to 30 s. For CO_2 plasma damage on OSG 2.4, there are two exceptional data points, 2 s and 5 s plasma exposures that show a stronger decrease in porosity.

Therefore, the accumulation of CO_2 molecules is the result of complete pore sealing, which allows for CO_2 to be trapped inside the pores of the materials. Here, there is no significant difference between CO_2 and O_2 plasma damage noticeable from the EP results.

Despite the absence of ion bombardment in the ICP-remote plasma chamber, the data presented show that the OSG 2.2 film suffers $SiCH_3$ depletion from O radicals diffusion, porosity reduction and consequently lesser damage by CO_2 plasma as opposed to O_2 plasma. The following distinctions can thus be made from the data presented in the ICP-remote plasma configuration:

- While structural modifications (from EP data) are more intense yet saturated after 20 s on OSG 2.2 for both plasma treatments, CO_2 plasma damage is not saturated on OSG 2.4.
- Chemical modifications (FTIR) are saturated after 5 s in CO_2 plasma for OSG 2.4 whereas the chemical modifications (FTIR) are not saturated after 30s in the CO_2 or O_2 plasma for OSG 2.2.

Summary

Generally in consistence with previous research,[5–12] O_2 plasma was found to be more damaging compared to CO_2 at short treatment times although the total carbon depletion is not so pronounced in both cases (Figure 4). The following new observations could be highlighted from the obtained results.

CCP-RIE CO_2 plasma efficiently and rapidly seals the OSG 2.4 surface. The sealing of OSG 2.2 film needs longer time because of its higher porosity and larger pore size. The sealing and CO_2 accumulation is also observed during CCP-RIE O_2 plasma as in CO_2 although it takes a longer time for sealing to occur. The sealing is consistent with earlier study.[24] The CO_2 accumulation in O_2 plasma is a clear indication that it is formed as a reaction product. The fact that the reaction products are still forming after sealing can be related to VUV light emitted by O_2 plasma. Electron impact excitation of O atoms generates O(3 s), O(5 s), and O(5 p) states. The O(3 s) emits 130 nm photons and O(5 s) emits 136 nm photons in relaxing to ground state.[27] It is necessary to mention that these wavelengths are located in the region of the most severe VUV induced damage to OSG materials.[28] VUV light breaks $SiCH_3$ bonds and forms CH_x radicals which react with residual H_2O that was formed as another reaction product of CH_x oxidation.

The porosity of the low-k films is also reduced in the ICP-remote plasma configuration despite the absence of ions. In addition, partial sealing and no CO_2 accumulation was observed. However, complete sealing was not achieved in these experiments.

The integral damage (total loss of $SiCH_3$ groups) in CO_2 and O_2 plasma are not very different (Figure 4). However, the difference is very clear from the TOFSIMS data (Figure 7). The depth of damage after short exposure in CO_2 and O_2 plasma was almost the same ($\approx$15 nm). In the case of CO_2 plasma further reduction of carbon concentration near the top surface is observed while the depth of damage remains unchanged. In the case of O_2 plasma in addition to reduction of surface carbon concentration significant damage propagation into the film is observed. After 60 s exposure the depth of damage was about 75 nm.

Degree of damage very much depends on plasma power (Figures 8, 9). The bulk damage can be characterized as the total loss of $SiCH_3$ groups and amount of adsorbed moisture. At plasma power of 50 W, the amount of adsorbed moisture is relatively small. However, water contact angle measurements shows efficient hydrophilization of the low-k surface. This observation is important for generation of surface active sites for SAM deposition and atomic layer deposition (ALD). It is proposed that a 2 s, 55 mT, 50/100 W CO_2 plasma is sufficient to make the surface of ultralow-k films hydrophilic as these conditions provide the least damage to the material i.e. the least C depletion.

References

1. M. R. Baklanov and K. Maex, *Philos. Trans. A. Math. Phys. Eng. Sci.*, **364**, 201 (2006) http://www.ncbi.nlm.nih.gov/pubmed/18272461.
2. M. R. Baklanov et. al., *J. Appl. Phys.*, **113**, 041101 (2013) http://link.aip.org/link/JAPIAU/v113/i4/p041101/s1&Agg=doi.
3. M. A. Worsley et. al., *J. Vac. Sci. Technol. B Microelectron. Nanom. Struct.*, **23**, 395 (2005) http://scitation.aip.org/content/avs/journal/jvstb/23/2/10.1116/1.1861038.
4. D. Shamiryan, M. R. Baklanov, S. Vanhaelemeersch, and K. Maex, *J. Vac. Sci. Technol. B Microelectron. Nanom. Struct.*, **20**, 1923 (2002) http://scitation.aip.org/content/avs/journal/jvstb/20/5/10.1116/1.1502699.
5. X. Hua et. al., *J. Vac. Sci. Technol. B Microelectron. Nanom. Struct.*, **24**, 1238 (2006) http://scitation.aip.org/content/avs/journal/jvstb/24/3/10.1116/1.2194947.
6. N. C. M. Fuller et. al., *Thin Solid Films*, **516**, 3558 (2008) http://linkinghub.elsevier.com/retrieve/pii/S0040609007015118.
7. Ming-Shu Kuo, PhD thesis, The University of Maryland (2010).
8. Hualiang Shi, PhD thesis, The University of Texas in Austin (2010).
9. M.-S. Kuo, A. R. Pal, G. S. Oehrlein, P. Lazzeri, and M. Anderle, *J. Vac. Sci. Technol. B Microelectron. Nanom. Struct.*, **28**, 952 (2010) http://scitation.aip.org/content/avs/journal/jvstb/28/5/10.1116/1.3482343.
10. M.-S. Kuo, A. R. Pal, G. S. Oehrlein, and X. Hua, *J. Vac. Sci. Technol. B Microelectron. Nanom. Struct.*, **28**, 961 (2010) http://scitation.aip.org/content/avs/journal/jvstb/28/5/10.1116/1.3482353.
11. M.-S. Kuo and G. S. Oehrlein, *J. Vac. Sci. Technol. B Microelectron. Nanom. Struct.*, **28**, 1104 (2010) http://scitation.aip.org/content/avs/journal/jvstb/28/6/10.1116/1.3499271.
12. H. Shi et. al., *J. Vac. Sci. Technol. B Microelectron. Nanom. Struct.*, **30**, 011206 (2012) http://scitation.aip.org/content/avs/journal/jvstb/30/1/10.1116/1.3671008.

13. H. Shi et. al., in *Advanced Interconnects for ULSI Technology*, M. Baklanov, P. Ho, and E. Zschech, Editors, John Wiley & Sons, Ltd. (2012).
14. V. Jousseaume, A. Zenasn, O. Gourhant, M. Baklanov, and L. Favennec, in *Advanced Interconnects for ULSI Technology*, M. Baklanov, P. Ho, and E. Zschech, Editors, John Wiley & Sons, Ltd. (2012).
15. T. Asefa, M. J. MacLachlan, N. Coombs, and G. A. Ozin, *Nature*, **402**, 867 (1999) http://dx.doi.org/10.1038/47229.
16. B. J. Melde, B. T. Holland, C. F. Blanford, and A. Stein, *Chem. Mater.*, **11**, 3302 (1999) http://pubs.acs.org/doi/abs/10.1021/cm9903935.
17. S. Inagaki, S. Guan, Y. Fukushima, T. Ohsuna, and O. Terasaki, *J. Am. Chem. Soc.*, **121**, 9611 (1999) http://pubs.acs.org/doi/abs/10.1021/ja9916658.
18. J. Dendooven et. al., *Langmuir*, **28**, 3852 (2012) http://www.ncbi.nlm.nih.gov/pubmed/22304361.
19. M. R. Baklanov, K. P. Mogilnikov, V. G. Polovinkin, and F. N. Dultsev, *J. Vac. Sci. Technol. B*, **18**, 1385 (2000) http://link.aip.org/link/JVTBD9/v18/i3/p1385/s1&Agg=doi.
20. D. Shamiryan, M. R. Baklanov, and K. Maex, *J. Vac. Sci. Technol. B Microelectron. Nanom. Struct.*, **21**, 220 (2003) http://link.aip.org/link/JVTBD9/v21/i1/p220/s1&Agg=doi.
21. A. Grill and D. a. Neumayer, *J. Appl. Phys.*, **94**, 6697 (2003) http://link.aip.org/link/JAPIAU/v94/i10/p6697/s1&Agg=doi.
22. E. Levrau et. al., *Langmuir*, **29**, 12284 (2013) http://www.ncbi.nlm.nih.gov/pubmed/24000800.
23. F. Bailly et. al., *J. Appl. Phys.*, **108**, 014906 (2010) http://scitation.aip.org/content/aip/journal/jap/108/1/10.1063/1.3446820.
24. E. Kunnen et. al., *J. Vac. Sci. Technol. B Microelectron. Nanom. Struct.*, **28**, 450 (2010) http://scitation.aip.org/content/avs/journal/jvstb/28/3/10.1116/1.3372838.
25. Y. Sun et. al., (to be published), *No Title*.
26. T. Frot et. al., *2011 IEEE Int. Interconnect Technol. Conf.*, 1 (2011) http://ieeexplore.ieee.org/lpdocs/epic03/wrapper.htm?arnumber=5940272.
27. J. Shoeb, M. M. Wang, and M. J. Kushner, *J. Vac. Sci. Technol. A Vacuum, Surfaces, Film.*, **30**, 041303 (2012) http://scitation.aip.org/content/avs/journal/jvsta/30/4/10.1116/1.4718444.
28. T. V Rakhimova et. al., *J. Phys. D. Appl. Phys.*, **47**, 025102 (2014) http://stacks.iop.org/0022–3727/47/i=2/a=025102?key=crossref.a639a6133f887bd79d9e101735244c5e.
29. http://www.sigmaaldrich.com/Brands/Aldrich/Tech_Bulletins/AL_143/Molecular_Sieves.html.